

New palladium complexes with rigid scorpion-type ligands. Crystal structure of complexes $[\text{Pd}(\eta^3\text{-2-CH}_3\text{-C}_3\text{H}_4)(\text{bpz}^*\text{mPh})](\text{CF}_3\text{SO}_3)$ and $[\text{Pd}(\text{bpz}^*\text{mpy})_2](\text{BF}_4)_2$.

bpz^*mPh = phenyl-bis(3,5-dimethylpyrazol-1-yl)methane;
 bpz^*mpy = pyridin-2-yl-bis(3,5-dimethylpyrazol-1-yl)methane

Nieves Arroyo, Felipe Gómez-de la Torre, Félix A. Jalón*, Blanca R. Manzano, B. Moreno-Lara, Ana M. Rodríguez

Departamento de Química Inorgánica, Orgánica y Bioquímica, Universidad de Castilla-La Mancha, Facultad de Químicas, Avda. Camilo J. Cela, 10, 13071 Ciudad Real, Spain

Received 21 December 1999; received in revised form 28 February 2000

Dedicated to Professor Elguero on the occasion of his 60th birthday for his outstanding contribution to chemistry and as an expression of personal gratitude to him

Abstract

Two α -R substituted bis(3,5-dimethylpyrazol-1-yl)methane ligands ($R = \text{Ph}$, bpz^*mPh and 2-py, bpz^*mpy) have been used to synthesise new palladium(II) compounds with the general formulae $\text{PdXX}'(\text{bpz}^*\text{mR})$ ($R = \text{Ph}$, $X = X' = \text{Cl}$; **1a**, $X = X' = \text{Me}$; **2a**, $X = \text{Cl}$, $X' = \text{Me}$; **3a**, $X = X' = \text{C}_6\text{F}_5$; **4a** or $R = 2\text{-py}$, $X = X' = \text{Cl}$; **1b**, $X = \text{Cl}$, $X' = \text{Me}$; **3b**, $X = X' = \text{C}_6\text{F}_5$, **4b**), $[\text{Pd}(\eta^3\text{-2-CH}_3\text{-C}_3\text{H}_4)(\text{bpz}^*\text{mR})]\text{X}$ ($X = \text{PF}_6^-$, $R = \text{Ph}$, **5a**; $X = \text{CF}_3\text{SO}_3^-$, 2-py, **5b**) and $[\text{Pd}(\text{bpz}^*\text{mR})_2](\text{BF}_4)_2$ ($R = \text{Ph}$, **6a**; 2-py, **6b**). In all the complexes the bpz^*mR ligands adopt a rigid conformation with the R group in an axial position and, as a consequence, no boat-to-boat interconversion is observed. In **1b** and **3b–5b** the pyridine group is uncoordinated. Complex **5b** is present as a single isomer, while **5a** exists as two isomers that are in equilibrium and differ in the orientation of the allyl group with respect to the NN ligand. For complex **6b** the four possible *anti* isomers are observed in solution. The molecular structures of the major isomer of **5a** and one of the isomers of **6b** have been determined by X-ray structure analysis. In both structures the bpz^*mR ligands are coordinated as bidentate. For **5a** the ligand backbone confirms the stated rigidity. For **6b** a pyridine–pyrazole coordination of the two bpz^*mpy ligands is observed. The fluxional behaviour implying interconversion of the two pyrazole rings in **3b**, of the two isomers in **5a** and the rotation of the C_6F_5 groups in **4a** and **4b** has also been studied. © 2000 Elsevier Science S.A. All rights reserved.

Keywords: Palladium; Bis-pyrazolylmethane; Rigidity; Fluxional behaviour; Scorpion

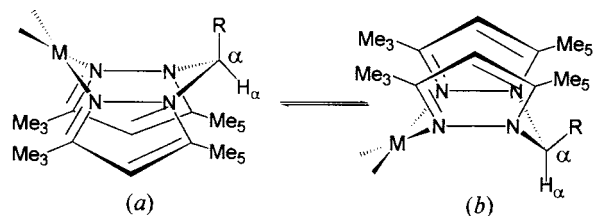
1. Introduction

Rigidity is one of the most desirable qualities of a ligand intended for certain specific catalytic uses such as, for example, polymerisation processes. This property is associated with the selectivity of a system in adopting only one of the different conformational or

configurational possibilities. A number of studies have been performed on bispyrazolylmethane [1] or borate [1–3] ligands coordinated to a metallic centre, and it was found that when a methine substituent is present, two conformations are expected (see Scheme 1) depending on the axial or equatorial disposition of the α -R substituent. In the present work, we prepared two α -substituted bis(3,5-dimethylpyrazol-1-yl)methane derivatives, phenyl-bis(3,5-dimethylpyrazol-1-yl)methane (bpz^*mPh) and pyridin-2-yl-bis(3,5-dimethyl-

* Corresponding author. Fax: +34-926-295318.

E-mail address: fjalón@qino-cr.uclm.es (F.A. Jalón)



R = Ph, bpz*mPh; 2-pyridine, bpz*mpy

Scheme 1.

pyrazol-1-yl)methane (bpz*mpy) (see Scheme 1), and explored their coordination abilities with different d^8 Pd fragments in order to evaluate the contribution of the α -R-substituent and the pyrazole methyl groups to the molecular rigidity of the ligand. The two conformers shown in Scheme 1 may be in a chemical exchange through a boat-to-boat inversion, but the steric hindrance of R and the Me₅ groups in conformer *b* could give rise to an unequal distribution of the population between the two conformations.

2. Results and discussion

2.1. Synthesis of ligands and complexes

Bpz*mPh [1] and bpz*mpy [4] were prepared by methods previously reported for related compounds. Complexes **1a**, **1b**, **3a**, **3b**, **4a**, **4b**, **6a** and **6b** were prepared by replacement of 1,5-cyclooctadiene (cod) or CH₃CN molecules in the appropriate Pd precursors by the pyrazole derivatives. The removal of chloride anions from the dimer [Pd(η^3 -2-CH₃-C₃H₄)Cl]₂ with a silver salt in a coordinating solvent, such as acetone, and the addition of the ligands led to the allyl derivatives. Complex **2a** was obtained by reaction of **1a** with methyllithium (see Scheme 2).

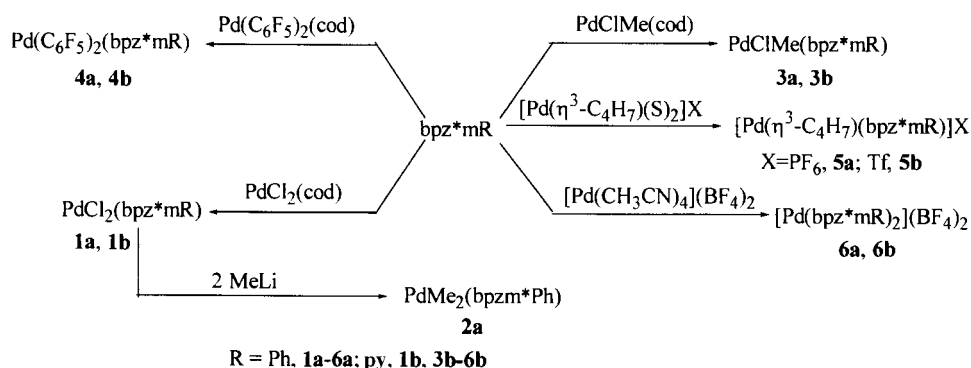
The complexes are soluble in polar solvents such as acetone, THF and dichloromethane and are stable under an atmosphere of nitrogen at room temperature

(r.t.), except complex **2a**, which decomposes slowly at this temperature. This complex reacts with halogenated solvents.

2.2. Characterisation of the new complexes

The IR spectra of the complexes are consistent with the presence of the nitrogen donor, ancillary ligands and the corresponding counteranions. Table 1 (¹H-NMR) and Table 2 (¹³C-NMR) show the chemical shifts and coupling constants for the free ligands and all the complexes, except for the mixture of isomers obtained for complex **6b**. The assignment of the signals was made by considering the chemical shifts and coupling constants expected for the different atoms and the information obtained from ¹H–¹H COSY experiments. The differentiation of Me₃ and Me₅ groups is based on the NOE observed for the whole set of complexes between Me₅ and the H _{α} protons and between one of the Me₃ groups and the Pd–Me group in **3a** and **3b** (see Scheme 3). The NOE between the H_{ortho} (Ph) or H₃ (py) signals and H _{α} was used to assign these resonances. A noticeable effect is the systematic difference observed (0.3–0.6 ppm) in the chemical shifts of the *ortho* protons of the Ph group when compared with the H₃ protons of the py fragment in both series of compounds. In the free ligands the chemical shifts of these protons are nearly identical. This behaviour could be due to the different population of the rotamers, which is related to the free rotation around the C _{α} –aryl bond. In the compounds containing the pyridine group, a weak interaction between the N atom and the anti-bonding orbital perpendicular to the coordination plane of the Pd centre could favour the corresponding rotamer, whereas in the bpz*mPh series this rotamer could be less probable for steric reasons.

Upon coordination, the proton and carbon resonances of the pyrazole groups are shifted to lower field, as is generally observed in coordinated heterocyclic rings. A particular effect is observed for **4a** and **4b**,



R = Ph. **1a-6a**: py. **1b, 3b-6b**

Scheme 2.

Table 1
¹H-NMR data for ligands and complexes ^a

Compound	Pyrazole		H _x	Ph or py group	Me–Pd or allylPd
	H ₄	Me			
bpz*mPh ^b	5.86	2.19 (Me ₃) 2.21 (Me ₅)	7.63	6.91 (m, H _o) 7.30 (m, H _{m,p})	
bpz*mpy ^b	5.88	2.18 (Me ₃) 2.21 (Me ₅)	7.57	6.92 (dd, J _{HH} = 7.8, 1.0, H ₃) 7.69 (td, J _{HH} = 7.8, 1.7, H ₄) 7.26 (dd, J _{HH} = 7.8, 4.9, H ₅) 8.64 (ddd, J _{HH} = 4.9, 1.7, 1.0, H ₆)	
PdCl ₂ (bpz*mPh) ^b (1a)	6.05	2.52 (Me ₃) 2.59 (Me ₅)	7.38	7.05 (m, H _o) 7.61 (m, H _{m,p})	
PdCl ₂ (bpz*mpy) ^b (1b)	6.04	2.54 (Me ₃) 2.58 (Me ₅)	7.27	7.63 (d, J _{HH} = 7.8, H ₃) 7.98 (td, J _{HH} = 7.8, 1.7, H ₄) 7.47 (dd, J _{HH} = 7.8, 4.6, H ₅) 8.71 (m, H ₆)	
PdMe ₂ (bpz*mPh) ^c (2a)	5.45	2.35 (Me ₃ , Me ₅)	6.72	6.69 (m, H _o) 7.18 (m, H _{m,p})	0.53
PdClMe(bpz*mPh) ^d (3a)	6.21 (H ₄) 6.04 ^e (H ₄)	2.31 (Me ₃) 2.66 (Me ₅) 2.40 ^e (Me ₃) 2.57 ^e (Me ₅)	7.82	6.80 (m, H _o) 7.38 (m, H _{m,p})	0.27
PdClMe(bpz*mpy) ^d (3b)	6.11	2.33 (Me ₃) 2.60 (Me ₅)	7.73	7.08 (d, J _{HH} = 7.8, H ₃) 7.80 (td, J _{HH} = 7.8, 1.6, H ₄) 7.40 (dd, J _{HH} = 7.8, 4.8, H ₅) 8.54 (d, J _{HH} = 4.8, H ₆)	0.23
PdClMe(bpz*mpy) ^d (3b) 183 K	6.25 (H ₄) 6.15 ^e (H ₄)	2.20 (Me ₃) 2.65 (Me ₅) 2.33 ^e (Me ₃) 2.60 ^e (Me ₅)	7.92	6.85 (d, H ₃) 7.83 (td, H ₄) 7.49 (dd, H ₅) 8.55 (d, H ₆)	0.09
Pd(C ₆ F ₅) ₂ (bpz*mPh) ^b (4a)	6.01	1.94 (Me ₃) 2.48 (Me ₅)	7.39	6.78 (m, H _o) 7.56 (m, H _{m,p})	
Pd(C ₆ F ₅) ₂ (bpz*mpy) ^b (4b)	6.01	1.94 (Me ₃) 2.51 (Me ₅)	7.32	7.11 (d, J _{HH} = 7.6, H ₃) 7.93 (t, J _{HH} = 7.6, H ₄) 7.47 (dd, J _{HH} = 7.6, 4.8, H ₅) 8.73 (d, J _{HH} = 4.8, H ₆)	
[(¹³ C ₄ H ₇)Pd(bpz*mPh)]PF ₆ ^d (5aM) 223 K	6.42	2.32 (Me ₃) 2.70 (Me ₅)	8.01	6.47 (m, H _o) 7.42 (m, H _{m,p})	3.88 (H _{syn}) 3.14 (H _{anti}) 1.14 (Me)
5am ^d 223 K	6.39	2.23 (Me ₃) 2.74 (Me ₅)	8.27	6.95 (m, H _o) 7.46 (m, H _{m,p})	4.16 (H _{syn}) 1.71 (H _{anti}) 2.15 (Me)
[(¹³ C ₄ H ₇)Pd(bpz*mpy)]Tf ^b (5b)	6.18	2.29 (Me ₃) 2.60 (Me ₅)	7.56	6.80 (dd, J _{HH} = 8.1, 1.0, H ₃) 7.83 (td, J _{HH} = 7.8, 2.0, H ₄) 7.31 (m, H ₅) 8.54 (dm, J _{HH} = 4.9, H ₆)	3.86 (H _{syn}) 2.71 (H _{anti}) 1.52 (Me)
[(¹³ C ₄ H ₇)Pd(bpz*mpy)]Tf ^d (5b) 183 K	6.36	2.32 (Me ₃) 2.69 (Me ₅)	7.97	6.82 (dd, H ₃) 7.90 (td, H ₄) 7.44 (ddt, J _{HH} = 7.8, 4.9, 1.0, H ₅) 8.56 (dm, H ₆)	3.99 (H _{syn}) 2.93 (H _{anti}) 1.52 (Me)
[Pd(bpz*mPh) ₂](BF ₄) ₂ ^d (6a)	6.46	1.92 (Me ₃) 2.75 (Me ₅)	8.28	7.43 (m, H _o) 7.74 (m, H _{m,p})	

^a At room temperature if not specified. Chemical shifts in ppm and coupling constants in Hz. All resonances are singlets if not specified. *o*, *m*, *p*: *ortho*, *meta* and *para*, respectively. d, doublet; t, triplet; m, multiplet.

^b CDCl₃.

^c C₆D₆.

^d (CD₃)₂CO.

^e Signals corresponding to pyrazolyl groups *trans* to Me.

where the Me₃ proton resonances are markedly shifted to higher field, probably as a consequence of the electron current anisotropy [5] of the C₆F₅ rings. This effect

has also been observed in protons of coordinated heterocyclic ligands situated close to metal aryls fragments [6].

Table 2
 $^{13}\text{C}\{^1\text{H}\}$ -NMR data for ligands and complexes ^a

Compound	Pyrazole			C_α	Phenyl or 2-pyridyl				Me-Pd or allylPd	
	C_4	Me_3, Me_5	C_3, C_5		C_{ortho}	C_{meta}	C_{para}	C_{ipso}		
bpz*mPh ^b	107.32	12.36	137.33	74.40	127.29	129.01	128.85	148.83		
1a ^b	108.36	11.47	134.05	69.27	126.62	129.77	130.66	155.04		
		14.27	141.54							
2a ^c	106.60	11.47	134.05	68.45		125.60–129.24 ^c		136.93	10.45	
		14.38	150.98							
3a ^b	107.13	10.99	139.77	68.49	126.34	128.99	129.55	135.42	–8.36	
		11.58	140.96							
		14.02	152.47							
		14.95	152.73							
4a ^d	108.79	11.44	144.71	69.82	126.74	129.95	129.76	135.82		
		13.91	153.83							
5^aM+5am ^d	108.28	11.26	^e	69.57	126.68	129.89	130.18	^e	59.79(CH ₂) 22.14 (Me)	
		14.88								
6a ^d	110.50	11.88	149.83	70.84	127.65	130.75	131.75	^e		
		15.14	155.89							
					C_2	C_3	C_4	C_5	C_6	
bpz*mpy ^b	106.85	11.39	140.70	74.57	155.58	123.12	136.8	122.22	149.43	
1b ^b	108.44	11.60	^e	69.73	^e	125.05	137.93	123.61	150.48	
		13.78	148.52							
3b ^d	107.71	11.29	143.80	70.34	155.71	124.36	137.52	124.06	149.83	–9.01
		14.45	152.71							
4b ^b	108.32	11.61	142.03	69.12	159.35	124.37	138.25	122.03	150.50	
		13.88	153.39							
5b ^b	107.66	11.55	144.28	69.02	153.22	124.32	137.96	122.19	149.95	59.37(CH ₂) 22.64 (Me) 131.41(–C=)
		15.04	152.69							

^a Room temperature. Chemical shifts in ppm. All signals are singlets.

^b CDCl₃.

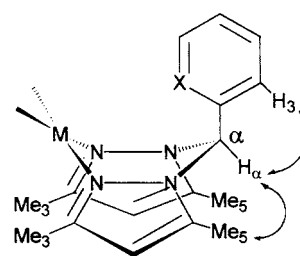
^c C₆D₆.

^d (CD₃)₂CO.

^e Non assigned or non-observed resonances.

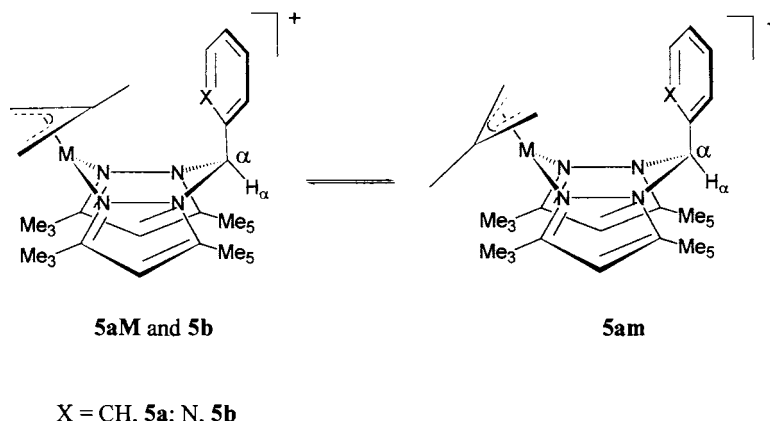
The aforementioned NOEs between neighbouring groups in these compounds (see Scheme 3) are in accordance with a rigid boat conformation for the metallacyclic ring with the R fragment in an axial disposition on the methine C_α group. Accordingly, given the rigidity of these ligands, the low temperature ^1H -NMR spectra of all complexes showed unchanged patterns. As a consequence, the boat-to-boat conformational exchange depicted in Scheme 1, which has been observed in non- α -substituted bis(3,5-Me₂-pyrazol-1-yl)methane and borate Pd derivatives [1], can be excluded in our complexes. It is very probable that the steric repulsion of the R group in the α position, with the two Me₅ fragments of the pyrazole rings, precludes the formation of conformer (b) in Scheme 1. This scorpion backbone of the ligand is, with some exceptions [7], the type normally observed in the solid state for similarly α -substituted bis(pyrazol-1-yl)methane derivatives and therefore it may be considered as the most stable situation for the metallacyclic ring.

This rigidity and the existence of the previously explained proximity between the α -R groups and the palladium centre could imply blockage of one of the perpendicular coordination positions of the palladium centre. This aspect is crucial to avoid substitution pro-



X = CH, **1a-6a**; N, **1b, 3b-5b**

Scheme 3. Main NOEs observed which establish the rigid conformation of the bpz*mR ligands.



Scheme 4.

cesses such as alkene exchange in catalytic polymerisation reactions. The exchange is undesirable for an extended chain propagation [8].

The equivalence of the two pyrazole rings in complexes **1b**, **4b** and **5b** above the melting points of the corresponding solvents (see Table 1) implies the uncoordination of the pyridine group. This conclusion is in contrast both with the more basic character of this heterocycle when compared with pyrazole and with the observations of other authors regarding non-substituted bpzmpy ligands coordinated to PdXX' fragments. For example, in PdIMe(bpzmpy) both isomers, pz₂Pd and pzpyPd, are observed in solution [4]. This implies a more specific coordination of the bpz*mpy ligand, which is an additional advantage for the rigidity of this scorpion-type ligand.

The ¹H- and ¹³C-NMR spectra of the allyl derivatives **5a** and **5b** show the symmetric environments expected for a C_s symmetry (see Tables 1 and 2). While **5b** is present as only one isomer both in (CD₃)₂CO and CDCl₃ solutions even at low temperature, **5a** exists, in the temperature range allowed in the deuterated solvents, in the form of two isomers in equilibrium (**5aM**:**5am**) in a variable ratio (always > 1, M = major, m = minor isomer) depending on the solvent used. These two isomers can be assigned to the two expected different orientations of the 2-Me-allyl group in the imposed symmetry of the Pd bpz*mR fragment, as depicted in Scheme 4. The existence of these types of isomers has been previously observed in other bis(pyrazol-1-yl)methane and borate complexes when the boat-to-boat interchange is frozen [1,9].

Complexes **5aM** and **5b** have identical structures, with the allylic methyl group pointing towards the α-substituent. This situation is deduced from the observed NOEs between the Me₃ group and the allylic protons (*syn* and *anti*), as well as the chemical shift of the allylic methyl groups in the ¹H-NMR spectrum. The signal due to the allylic methyl is shifted to significantly higher field (see Table 1) as a consequence of the

shielding of the Ph or 2-py groups in the rigid conformation of the bpz*mR ligand. In the isomer **5am** the chemical shift of the allylic methyl is in the usual region but the H_{anti} protons are now especially shielded. This shielding effect of the ligand bpz*mPh on an allylic group has been previously observed in a molybdenum complex [10]. In our case, this hypothesis was confirmed after the determination of the molecular structure of **5aM** by an X-ray diffraction study.

Crystals of the cationic complex **5aM** belong to the orthorhombic space group *Pnma* and the molecular structure consists of a mononuclear Pd cation and a triflate counterion. The cation lies on a crystallographic mirror plane containing Pd(1), C(2), C(3), C(10) and C(13), and consequently only half of the molecule is crystallographically independent. An ORTEP plot of the cation is shown in Fig. 1 and the crystallographic data and a selected list of bond distances and angles are given in Tables 3 and 4, respectively. The geometry around the Pd(1) atom is approximately square-planar

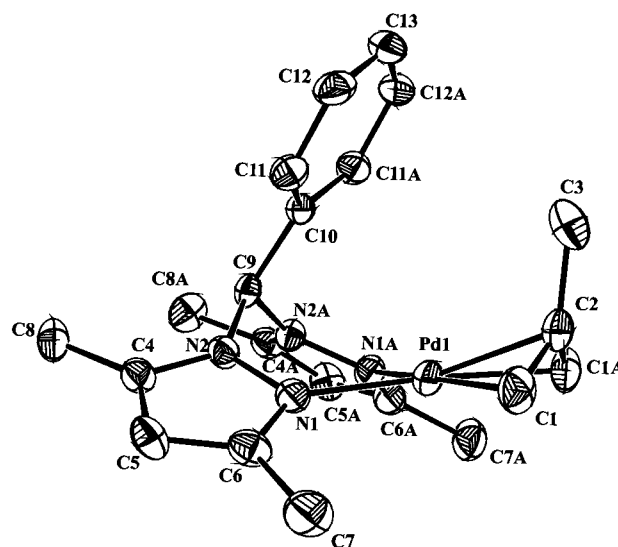
Fig. 1. Molecular structure of the cation of complex **5aM**.

Table 3
Crystal data and structure refinement for **5aM** and **6b**

	5aM	6b
Empirical formula	C ₂₁ H ₂₇ N ₄ Pd·CF ₃ SO ₃	C ₃₂ H ₃₈ N ₁₀ Pd·B ₂ F ₈
Formula weight	590.94	842.74
Temperature (K)	293(2)	293(2)
Wavelength (Å)	0.71070	0.71070
Crystal system	Orthorhombic	Monoclinic
Space group	<i>Pnma</i>	<i>I2/a</i>
<i>a</i> (Å)	17.058(3)	13.166(6)
<i>b</i> (Å)	10.773(7)	14.107(1)
<i>c</i> (Å)	13.487(1)	19.690(2)
β (°)		100.14(2)
Volume (Å ³)	2478.4(17)	3600.0(17)
<i>Z</i>	4	4
<i>D</i> _{calc} (g cm ⁻³)	1.584	1.555
Absorption coefficient (cm ⁻¹)	8.86	5.97
<i>F</i> (000)	1200	1712
Crystal size (mm)	0.4 × 0.4 × 0.2	0.4 × 0.3 × 0.3
Limiting indices	0 ≤ <i>h</i> ≤ 22, 0 ≤ <i>k</i> ≤ 14, 0 ≤ <i>l</i> ≤ 17	0 ≤ <i>h</i> ≤ 17, 0 ≤ <i>k</i> ≤ 18, -25 ≤ <i>l</i> ≤ 25
Data/restraints/parameters	3134/21/207	4337/27/278
Goodness-of-fit on <i>F</i> ²	0.959	0.836
Final <i>R</i> indices [<i>I</i> > 2σ(<i>I</i>)] ^a	<i>R</i> ₁ = 0.0435, <i>wR</i> ₂ = 0.0937	<i>R</i> ₁ = 0.0341, <i>wR</i> ₂ = 0.0933
<i>R</i> indices (all data)	<i>R</i> ₁ = 0.0871, <i>wR</i> ₂ = 0.1227	<i>R</i> ₁ = 0.0493, <i>wR</i> ₂ = 0.1077
Largest difference peak and hole (e Å ⁻³)	0.614 and -0.741	0.424 and -0.338

$$^a R_1 = \frac{\sum |F_o| - |F_c|}{\sum |F_o|}; wR_2 = \frac{[\sum (w(F_o^2 - F_c^2))^2]}{[\sum (w(F_o^2))^2]}^{1/2}.$$

Table 4
Selected bond lengths (Å) and angles (°) for complexes **5aM** and **6b**

5aM	6b		
Pd(1)–C(1)	2.111(5)	Pd(1)–N(1)	2.009(2)
Pd(1)–N(1)	2.115(4)	Pd(1)–N(5)	2.035(2)
Pd(1)–C(2)	2.123(7)	N(1A) ^b –Pd(1)–N(1)	95.54(12)
C(1)–C(2)	1.392(6)	N(1)–Pd(1)–N(5)	85.59(8)
C(2)–C(3)	1.523(11)	N(5A) ^b –Pd(1)–N(5)	93.28(12)
C(1A) ^a –Pd(1)–C(1)	67.6(3)	N(1)–N(2)–C(11)	120.54(19)
C(1)–Pd(1)–N(1)	102.30(18)	C(12)–N(5)–Pd(1)	120.47(17)
N(1A) ^a –Pd(1)–N(1)	87.67(19)	N(2)–C(11)–C(12)	109.6(2)
N(2)–N(1)–Pd(1)	118.6(3)	N(5)–C(12)–C(11)	117.8(2)
N(1)–N(2)–C(9)	119.1(4)		
C(1A) ^a –C(2)–C(1)	115.0(7)		
N(2)–C(9)–N(2A) ^a	111.1(5)		
N(2)–C(9)–C(10)	112.8(3)		

^a *x*, -*y*+1/2, *z*.

^b -*x*+1/2, *y*, -*z*.

with two coordinated pyrazole rings and the η³-bonded allyl ligand. The Pd(1)–N(1) and Pd(1)–C(1) distances are 2.115(4) and 2.111(5) Å, respectively.

The coordination of the bpz*mPh ligand gives rise to a metallacycle, Pd(1)(NN)₂C(9), with a boat conformation in which the phenyl group attached to the carbon atom C(9) is located in an axial position, the situation that has been established to occur in solution. The methyl allylic group has a *syn* orientation with respect to the phenyl ring, as emphasised in Fig. 2. This is the same disposition found by NMR studies in solution and produces the shielding effect previously stated.

If we define a plane containing the Pd and the two nitrogen atoms N(1) and N(1A), then the terminal allylic carbons are 0.105(4) Å below this plane and the central allylic carbon is 0.584(7) Å above it. The plane of the allyl group makes an angle of 112.9(5)° with the coordination plane in such a way that the C(central) to -CH₃ vector is pointing away from the metal.

The ¹H- and ¹³C-NMR spectra of complex **6a** both show a very simple pattern corresponding to a single, symmetrical disposition of the two coordinated bpz*mPh ligands. Considering the rigid character of this ligand, two different stereoisomers are possible (*syn* and *anti*, see Scheme 5) given the relative orientation of the rigid boat conformation of the ligands on the square plane of the palladium centre. Taking into account the resolved molecular structure for this type of compound [11] and the steric requirements of the pyrazole substituents in the 3-position, the *syn* isomer can be excluded.

A relevant aspect in the *anti* isomer is the special situation of the Me₃ pyrazole substituents, which are located at the face of the α-Ph group of the other bpz*mPh ligand, a situation that leads to a remarkable shielding of this methyl resonance in the ¹H-NMR spectrum (see Table 1).

In contrast with the very simple ¹H- and ¹³C-NMR spectra of complex **6a**, those of complex **6b** show a

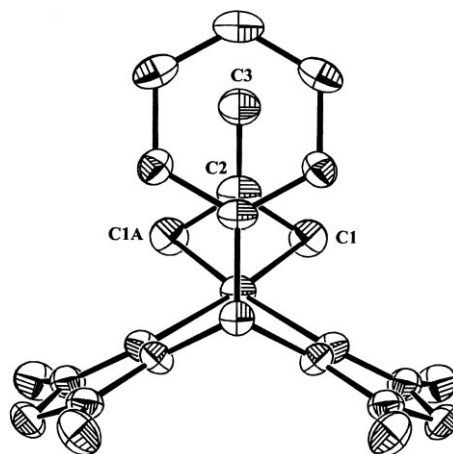
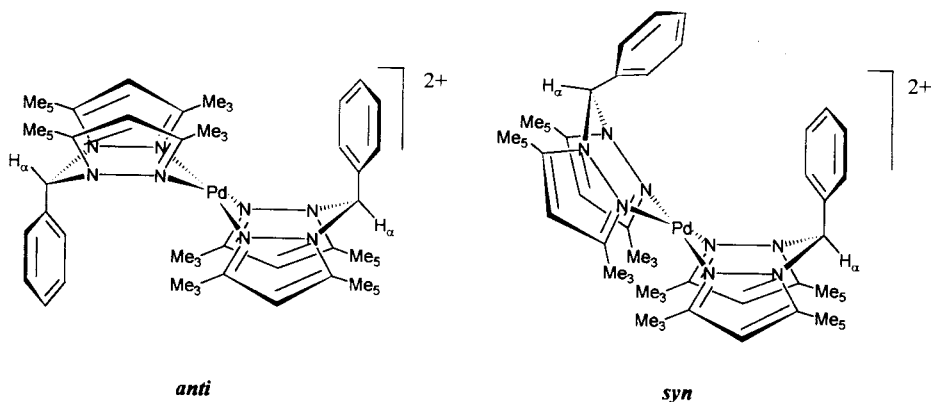
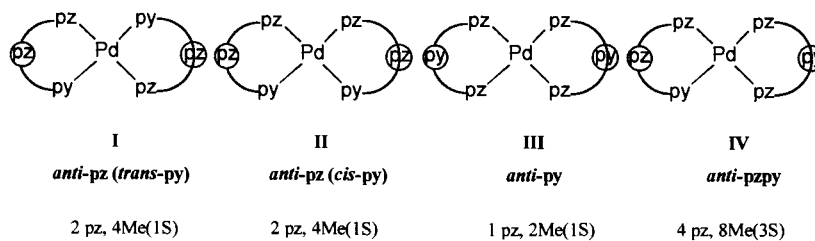


Fig. 2. Molecular projection showing the shielding effect of the phenyl group over the allylic methyl in the cation of **5aM**.



Scheme 5.

Scheme 6. Possible *anti* coordination isomers of **6b**.

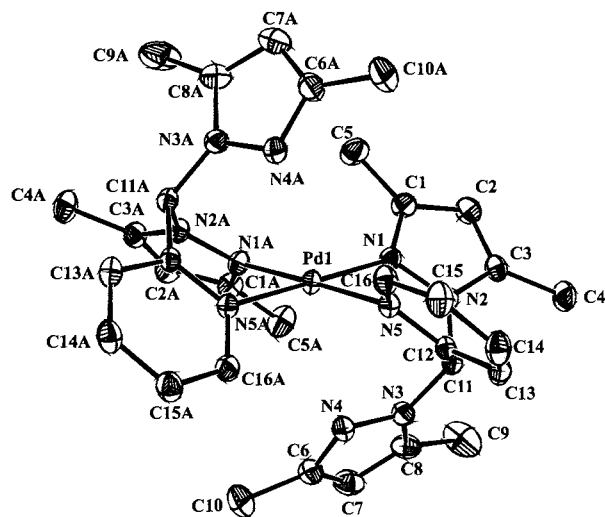
complicated distribution of isomers. This is a consequence of competition between the pyrazole and pyridine heterocycles of the two coordinated ligands for coordination to the palladium centre.

Assuming that the *syn* stereoisomers are less likely than the *anti*, due to the aforementioned steric hindrance of the Me₃ substituents, the number of possible *anti* isomers is four. These possibilities are depicted in Scheme 6.

The number of different pyrazole and methyl groups expected for each isomer is indicated below the structures in Scheme 6. In these *anti* isomers the uncoordinated α -R substituent should shield the Me₃ pyrazole group situated at its face and, as such, six shielded methyl resonances (indicated in parenthesis with the symbol S for each isomer) are expected if the four isomers I–IV are present. In practice six resonances, three of which of the same intensity due to shielded methyl groups (1.47–2.00 ppm), are observed in the corresponding ¹H-NMR spectrum. When the mixture is allowed to stand for a long period of time (1 month) a marked increase in the intensity of one shielded methyl resonance together with three non-shielded methyl resonances is observed. This corresponds to an enrichment in the mixture of isomer I or II and, consequently, one of these is the most thermodynamically stable. A decrease in the signals of equal intensity due to three shielded methyl groups is also observed, which indicates that isomer IV is now present to a lesser extent. A clear change in the signals of the other two isomers is not observed.

In order to elucidate several aspects of the coordination of the bpz*mpy ligand to the Pd centre, monocrystals of this isomeric mixture were obtained. The molecular structure determined by an X-ray diffraction study showed the presence of isomer II. The corresponding ORTEP diagram is shown in Fig. 3 and the crystallographic data as well as selected distances and bond angles are given in Tables 3 and 4, respectively.

Crystals of the cationic complex **6b** belong to the monoclinic space group *I*2/a. The asymmetric unit contains one half-molecule of the [Pd(bpz*mpy)₂] cation

Fig. 3. Molecular structure of the cation of complex **6b**.

with the Pd centre sitting on a C2 axis. There is also one BF_4^- counteranion per half-molecule. The two neutral ligands are coordinated in a bidentate fashion through the nitrogen atoms of one pyrazole and the pyridine rings. The two coordinated pyridine groups are in a mutually *cis* disposition. The coordination environment shows the Pd(1)–N(1) distance to be 2.009(2) Å and the Pd(1)–N(5) distance to be 2.035(2) Å.

The metallacycle Pd(1)(NN)(NC)C(11) has a boat conformation in which the two pyrazole groups attached to the carbon atoms C(11) are located in a mutually *anti* disposition. The dihedral angle between each free pyrazole ring and the palladium coordination plane is 123.6(1)°. In this situation the N(4) atom of the pyrazole is at a non-bonded N(4)··Pd(1) separation of 2.876(3) Å. The Me_3 group of the coordinated pyrazoles (C(5) and C(5A) in Fig. 3) is situated at the face of the free pyrazolyl ring of the other ligand. This is in accordance with the shielding observed in solution for these methyl groups.

2.3. Fluxional behaviour of several complexes

In contrast with the static behaviour observed in complex **3a** (from 183 to 323 K), which exhibits two different pyrazole groups, **3b** shows an apparent symmetric environment with two identical pyrazole rings at r.t. both in the ^1H - and ^{13}C -NMR spectra in acetone- d_6 . However, at low temperature (see Table 1) two clearly different pyrazole units are observed in the ^1H -NMR spectrum in accordance with the C_1 symmetry of this compound. The free activation energy for the exchange between the two pyrazole rings is 58.7 kJ mol $^{-1}$ at 263 K (calculated from the coalescence of the H_4 pyrazole protons). This noticeable difference in the activation barrier can be ascribed to the presence of the pyridine ring in **3b** but not in **3a**. The easy exchange of free and coordinated pyrazole fragments in tris(pyrazol-1-yl)methane and borate derivatives of Pd(II) has been previously observed [1,12,13] and such a tumbling process is thought to occur through pentacoordinated intermediates with the pyrazole ligand being tricoordinated to the metallic centre [14]. In complex **3b** the pyridine coordination could give rise to the pentacoordinate intermediate. The energy barrier for the tumbling process in tris(pyrazol-1-yl)methane and borate derivatives is especially low and in some cases the process is beyond the NMR time scale. In the case of complex **3b** this barrier is considerably higher and this should correspond to greater instability of the pentacoordinate intermediate. The absence of an α -R substituent with coordination ability in the bpz*mPh complexes, particularly in **3a**, precludes this exchange process.

As previously stated, two isomers of **5a** exist in solution: **5aM** and **5am**. They are in a dynamic equilibrium at r.t. both in $(\text{CD}_3)_2\text{CO}$ and CDCl_3 solution. The broad resonances of the ^1H -NMR spectra and the apparent existence of resonances for only one isomer in the ^{13}C -NMR spectrum suggest the existence of this exchange equilibrium. At low temperature, the ^1H -NMR spectrum shows the expected narrow resonances for the two isomers. Additional experiments indicate clearly the existence of this exchange since the irradiation of signals such as the allylic protons of the major isomer produces magnetisation transfer over the exchanging protons of the minor component. The limit imposed by the boiling point of the stated solvents has prevented the observation of any coalescence and the kinetic parameters of this exchange have been calculated in CDCl_2 – CDCl_2 . The obtained ΔG_c^\ddagger values for the different reached coalescences are in between 66.0/305 and 66.6/325 (kJ mol $^{-1}$ /K). This type of exchange has been observed both by ourselves and other authors in allyl derivatives of Pd(II) and the corresponding mechanism is thought to proceed via tricoordinate [15] or pentacoordinate [16] intermediates.

The ^{19}F -NMR spectra of complexes **4a** and **4b** in acetone solution at r.t. are quite comparable. Single resonances for the *ortho* (broad), *meta* and *para* fluorines are observed for **4a**, whereas two *ortho* resonances are observed for **4b**. When the temperature is decreased the single resonances of the *ortho* and *meta* fluoro substituents split to give different signals and, at low temperature, the pattern expected for two identical C_6F_5 groups with restricted rotation is observed. This behaviour is not unexpected considering the steric hindrance in the coordination environment of the Pd centre [17].

In both compounds, the two *ortho* fluorine resonances observed at low temperature have a different appearance. This should be due to the second order spin system arising from the couplings with the *meta* fluoro substituent, as demonstrated by homonuclear irradiation, and no evidence for an inter-ring coupling was observed [17a]. Considering the coalescences of the F_o resonances, the free energies of activation at the coalescence temperatures were estimated: (ΔG_c^\ddagger (kJ mol $^{-1}$)/T (K): 53.9/283 for **4a** and 57.1/311 for **4b**). If the pyridine group would participate in the rotational process of **4b**, the more plausible way would be by the formation of a pentacoordinate intermediate through the coordination of this heterocycle, a fact that is not possible in **4a**. This previsibly would lead to a decrease in the ΔG_c^\ddagger value. Considering that ΔG_c^\ddagger (**4b**) > ΔG_c^\ddagger (**4a**) (a high influence of the temperature is not expected) we propose that there is not a clear participation of the pyridine fragment in the rotational process.

3. Experimental

3.1. Starting materials and general conditions

3.1.1. General comments

All manipulations were carried out under an atmosphere of dry oxygen-free nitrogen using standard Schlenk techniques. Solvents were distilled from the appropriate drying agents and degassed before use. $[\text{Pd}(\eta^3\text{-2-Me-C}_3\text{H}_4)(\mu\text{-Cl})_2]$ [18], $[\text{Pd}(\text{C}_6\text{F}_5)_2(\text{cod})]$ [19], $[\text{PdCl}_2(\text{cod})]$ [20], $[\text{PdClMe}(\text{cod})]$ [21] and $[\text{Pd}(\text{CH}_3\text{CN})_4](\text{BF}_4)_2$ [22] were prepared as described in the literature. Elemental analyses were performed with a Perkin–Elmer 2400 micro analyser. IR spectra were recorded as KBr pellets or Nujol mulls with a Perkin–Elmer PE 883 IR spectrometer. ^1H - and ^{13}C -NMR spectra were recorded on a VARIAN UNITY 300 spectrometer. Chemical shifts (ppm) are given relative to TMS (^{13}C and ^1H) or CF_3Cl (^{19}F). COSY spectra: standard pulse sequence with an acquisition time of 0.214 s, pulse width 10 ms, relaxation delay 1 s, number of scans 16, number of increments 512. The NOE difference spectra were recorded with the following acquisition parameters: spectral width 5000 Hz, acquisition time 3.27 s, pulse width 18 ms, relaxation delay 4 s, irradiation power 5–10 dB, number of scans 240. For variable temperature spectra the probe temperature (± 1 K) was controlled by a standard unit calibrated with a methanol reference. Free energies of activation were calculated [23] from the coalescence temperature (T_c) and the frequency difference between the coalescing signals (extrapolated at the coalescence temperature) with the formula $\Delta G^\ddagger = aT[9.972 + \log(T/\delta\nu)]$, $a = 1.914 \times 10^{-2}$. The estimated error in the calculated free energies of activation is ± 0.5 kJ mol $^{-1}$.

3.1.2. X-ray structural determination of **5aM** and **6b**

Crystal, data collection, and refinement parameters are collected in Table 3. Suitable prismatic and colourless crystals of both complexes were selected and mounted on fine glass fibers with epoxy cement. The unit cell parameters were each determined from the angular setting of least-squares fit of 25 strong high-angle reflections. The asymmetric unit for **5aM** and **6b** contained half-independent molecule. Reflections were collected at 25°C on a NONIUS-MACH3 diffractometer equipped with a graphite monochromated radiation ($\lambda = 0.7107$ cm $^{-1}$). Each sample showed no significant intensity decay over the duration of data collection.

Data were corrected in the usual fashion for Lorentz and polarisation effects and empirical absorption correction was not necessary ($\mu = 8.86$ cm $^{-1}$ (**5aM**) and 5.97 cm $^{-1}$ (**6b**)). The space group was determined from the systematic absences in the diffraction data. The structures were solved by direct methods (SHELXS for **5aM** and SIR92 for **6b**) [24,25] and refinement on F^2

was carried out by full-matrix least-squares analysis (SHELXL-97) [24]. Anisotropic temperature parameters were considered for all non-hydrogen atoms, while hydrogen atoms were included in calculated positions but not refined. For **5aM** the triflate anion is disordered over two positions with identical occupancies.

3.2. Preparations

3.2.1.

Pyridin-2-yl-bis(3,5-dimethylpyrazol-1-yl)methane (bpz*mPy)

This ligand was prepared by a similar method [4] to that described for pyridin-2-yl-bis(pyrazol-1-yl)methane but using 3,5-dimethylpyrazole as starting reactive. Yield: 58%. $\text{C}_{16}\text{H}_{19}\text{N}_5$ (281.16): C, 68.34; H, 6.76; N, 24.89. Found: C, 68.32; H, 7.01; N, 24.72%.

3.2.2. $[\text{PdCl}_2(\text{bpz*mPh})]$ (**1a**)

To a solution of $\text{PdCl}_2(\text{cod})$ (0.80 g, 0.28 mmol) in 20 ml of dichloromethane, bpz*mPh was added (0.78 g, 0.28 mmol). The resulting yellow solution was stirred for 16 h until the formation of an orange colour. The resulting orange solid obtained after evaporation to dryness was washed with diethyl ether (2×5 ml). The solid was recrystallised from 1,2-dichloroethane–diethylether and orange crystals were obtained. Yield 86%. $\text{C}_{17}\text{H}_{20}\text{Cl}_2\text{N}_4\text{Pd}$ (457.49): Calc. C, 44.63; H, 4.37; N, 12.24. Found: C, 44.61; H, 4.30; N, 12.34%. IR (cm $^{-1}$) (Nujol): 1556 (C = Npz); 346, 331 (Pd–Cl).

3.2.3. $[\text{PdCl}_2(\text{bpz*mPy})]$ (**1b**)

A similar procedure to that used for **1a** was followed for **1b**. The reaction was made in acetone for 4 h. Yield 91%. $\text{C}_{16}\text{H}_{19}\text{Cl}_2\text{N}_5\text{Pd}$ (458.48): Calc. C, 41.90; H, 4.17; N, 15.27. Found: C, 41.65; H, 3.44; N, 15.23%. IR (cm $^{-1}$) (Nujol): 1583 (C = Npy); 1553 (C = Npz); 346, 332 (Pd–Cl).

3.2.4. $[\text{PdMe}_2(\text{bpz*mPh})]$ (**2a**)

A suspension of **1a** (0.82 g, 0.18 mmol) in 20 ml of diethyl ether was kept cold (-30°C) and 220 ml of a 1.6 M MeLi solution was added. The temperature was allowed to increase up to 0°C and then the solution was kept at this temperature for 30 min. Degassed cold water (1 ml) was added. The organic phase was separated in a separatory funnel and dried with Na_2SO_4 . The colourless solution was filtrated and evaporated to dryness. A pale yellow powdered solid was obtained. Yield 30%. The presence of some impurities of palladium metal makes this product unsuitable for a correct microanalysis.

3.2.5. $[\text{PdClMe}(\text{bpz*mPh})]$ (**3a**)

To a solution of $\text{PdClMe}(\text{cod})$ (0.2 g, 0.75 mmol) in 30 ml of toluene, bpz*mPh was added (0.21 mg, 0.75

mmol). The resulting solution was allowed to react for 6 h. A green pale solid was obtained after evaporation to dryness. This solid was recrystallised from THF–diethyl ether and pale yellow crystals were obtained. Yield 82%. $C_{18}H_{23}ClN_4Pd$ (437.05): Calc. C, 49.46; H, 5.26; N, 12.81. Found: C, 49.24; H, 4.96; N, 12.79%. IR (cm^{-1}) (Nujol): 1557 (C = Npz), 308 (Pd–Cl).

3.2.6. $[PdClMe(bpz*mpy)] \cdot 1/2C_4H_8O$ **3b**· $1/2C_4H_8O$

A similar procedure to that used for **3a** was followed for the synthesis of **3b**. The reaction was made in tetrahydrofuran for 2 h. Yield 89%. $C_{17}H_{22}ClN_5Pd \cdot 1/2C_4H_8O$ (474.06): Calc. C, 48.11; H, 5.52; N, 14.76. Found: C, 47.89; H, 4.94; N, 14.67%. IR (cm^{-1}) (Nujol): 1585 (C = Npy), 1555 (C = Npz), 318 (Pd–Cl).

3.2.7. $[Pd(C_6F_5)_2(bpz*mPh)]$ (**4a**)

To a solution of $Pd(C_6F_5)_2(cod)$ (0.8 g, 0.15 mmol) in 20 ml of dichloromethane, $bpz*mPh$ (0.41 g, 0.15 mmol) was added. The resulting solution was stirred for 16 h and a white solid was obtained after evaporation to dryness. Colourless crystals could be obtained from recrystallisation from 1,2-dichloroethane–pentane. Yield 84%. $C_{29}H_{20}F_{10}N_4Pd$ (720.71): Calc. C, 48.32; H, 2.78; N, 7.77. Found: C, 48.61; H, 2.60; N, 7.83%. ^{19}F -NMR ($CDCl_3$), r.t. δ –114.47 (bs, F_o); –162.91 (t, $J_{FF} = 21.4$ Hz, F_p); –165.68 (m, F_m); 213 K, δ –114.38 (m, F_o), –115.11 (m, F_o); –162.91 (t, $J_{FF} = 21.4$ Hz, F_p); –165.10 (m, F_m), –164.82 (m, F_m). IR (cm^{-1}) (Nujol): 1564 (C = Npz); 1625, 1498, 1059, 958 (C_6F_5).

3.2.8. $[Pd(C_6F_5)_2(bpz*mpy)] \cdot CH_2Cl_2$ **4b**· CH_2Cl_2

A similar procedure to **4a** was followed for **4b**. The reaction was carried out in acetone for 6 h. The product was recrystallised from dichloromethane. Yield 77%. $C_{28}H_{19}F_{10}N_5Pd \cdot CH_2Cl_2$ (806.84): Calc. C, 43.17; H, 2.62; N, 8.68. Found: C, 43.38; H, 2.34; N, 8.93%. ^{19}F -NMR, ($CDCl_3$), r.t. δ –113.93, –116.35 (bs, F_o); –162.81 (t, $J_{FF} = 21.4$ Hz, F_p); –165.56 (m, F_m); 213 K: δ –114.57 (m, F_o), –116.41 (m, F_o); –161.08 (t, $J_{FF} = 21.4$ Hz, F_p); –164.68 (m, F_m), –164.99 (m, F_m). IR (cm^{-1}) (Nujol): 1595 (C = Npy), 1567 (C = Npz); 1634, 1503, 1063, 960 (C_6F_5).

3.2.9. $[Pd(\eta^3-C_4H_7)(bpz*mPh)]PF_6$ (**5a**)

To a solution of $[Pd(\eta^3-C_4H_7)(\mu-Cl)]_2$ (200.00 mg, 0.5 mmol) in 20 ml of THF, $AgPF_6$ (256.74 mg, 1.0 mmol) was added. The solution was stirred at r.t. for 4 h and the resulting suspension was filtered off. Then $bpz*mPh$ (284.70 mg, 1.00 mmol) was added to the filtrate. After stirring for 1 h, the colourless solution thus formed was evaporated to dryness. The resulting white solid was washed with diethyl ether (2×20 ml). White crystals were obtained after a recrystallisation

from 1,2-dichloroethane–diethyl ether. Suitable crystals for X-ray diffraction were obtained in a similar way with $CF_3SO_3^-$ as counteranion. Yield: 84%. $C_{21}H_{27}F_6N_4PPd$ (586.61): Calc. C, 42.98; H, 4.60; N, 9.50. Found: C, 43.20; H, 4.42; N, 9.77%. IR (cm^{-1}) (KBr): 1571 (C = Npz); 748, 495 (PF_6).

3.2.10. $[Pd(\eta^3-C_4H_7)(bpz*mpy)]Tf$ (**5b**)

A similar procedure to **5a** was followed for **5b**. The reaction was made in acetone for 4 h and the recrystallisation from acetone–diethyl ether. Yield 86%. $C_{21}H_{24}F_3N_5O_3SPd$. (589.63): Calc. C, 42.61; H, 4.07; N, 11.83. Found: C, 42.52; H, 3.74; N, 11.95%. IR (cm^{-1}) (KBr): 1590 (C = Npy), 1565 (C = Npz); 1265, 1147, 771, 638 (CF_3SO_3).

3.2.11. $[Pd(bpz*mPh)_2](BF_4)_2$ (**6a**)

To a solution of $[Pd(CH_3CN)_4](BF_4)_2$ (47.37 mg, 0.11 mmol) in 10 ml of acetone, $bpz*mPh$ (60.00 mg, 0.21 mmol) was added. The solution was stirred at r.t. for 5 min and the resulting solution was evaporated to dryness. The resulting white solid was washed with diethyl ether (2×10 ml). White crystals were obtained after a recrystallisation from acetone–diethyl ether. Yield: 89%. $C_{34}H_{40}B_2F_8N_8Pd$ (840.38): Calc. C, 48.59; H, 4.76; N, 13.33. Found: C, 48.84; H, 5.25; N, 14.08%. IR (cm^{-1}) (Nujol): 1558 (C = Npz); 1055 (BF_4).

3.2.12. $[Pd(bpz*mpy)_2](BF_4)_2$ (**6b**)

A similar procedure to that used for **6a** was followed to obtain **6b**. Yield 84%. $C_{32}H_{38}B_2F_8N_{10}Pd$ (842.77): Calc. C, 45.61; H, 4.55; N, 16.62. Found: C, 45.99; H, 4.28; N, 17.10%. IR (cm^{-1}) (Nujol): 1603 (C = Npy), 1560 (C = Npz); 1065 (BF_4).

4. Supplementary material

Crystallographic data for the structural analysis have been deposited in the Cambridge Crystallographic Data Centre, CCDC no. 138315 for compound **5aM** and no. 138316 for compound **6b**. Copies of this information may be obtained free of charge from The Director, CCDC, 12 Union Road, Cambridge CB2 1EZ (Fax: +44-1223-336033; or e-mail: deposit@ccdc.ac.uk or <http://www.ccdc.cam.ac.uk>).

Acknowledgements

We gratefully acknowledge financial support from the Dirección General de Investigación Científica y Técnica (DGICYT) (Grant no. PB98-0315) of Spain and Professor Trofimenko for instructive discussions.

References

- [1] P.K. Byers, A.J. Canty, R.T. Honeyman, *Adv. Organomet. Chem.* 34 (1992) 1.
- [2] A. Shaver, in: G. Wilkinson (Ed.), *Comprehensive Coordination Chemistry*, vol. 2, Pergamon, Oxford, 1987, p. 245.
- [3] S. Trofimenko, *Scorpionates*, Imperian College Press, London, 1999.
- [4] P.K. Byers, A.J. Canty, R.T. Honeyman, *J. Organomet. Chem.* 385 (1990) 417.
- [5] I. Alkorta, J. Elguero, *New J. Chem.* (1998) 381.
- [6] For a discussion about this effect in complexes see: (a) G. Orellana, C. Alvarez-Ibarra, J. Santoro, *Inorg. Chem.* 27 (1988) 1025. (b) P.J. Steel, E.C. Constable, *J. Chem. Soc. Dalton Trans.* (1990) 1389.
- [7] A.J. Canty, J.L. Hoare, B.W. Skelton, A.H. White, G. van Koten, *J. Organomet. Chem.* 552 (1998) 23.
- [8] L. Deng, T.K. Woo, L. Cavallo, P.M. Margl, T. Ziegler, *J. Am. Chem. Soc.* 119 (1997) 6177.
- [9] F.A. Jalón, B.R. Manzano, F. Gómez de la Torre, A.M. Guerrero, A.M. Rodríguez, in: O.A. Attanasi, D. Spinelli (Eds.), *Targets in Heterocyclic Systems*, Società Chimica Italiana, Roma, 1999, v. 3.
- [10] K.-B. Shiu, Ch.-J. Chang, S.-L. Wang, F.-L. Liao, *J. Organomet. Chem.* 407 (1991) 225.
- [11] A.J. Canty, N.J. Minchin, L.M. Engelhardt, B.W. Skelton, A.H. White, *J. Chem. Soc. Dalton Trans.* (1986) 645.
- [12] (a) S. Trofimenko, *J. Am. Chem. Soc.* 92 (1970) 5118. (b) S. Trofimenko, *J. Am. Chem. Soc.* 88 (1966) 1842.
- [13] F.A. Jalón, B.R. Manzano, A. Otero, M.C. Rodríguez-Pérez, *J. Organomet. Chem.* 494 (1995) 179.
- [14] S. Trofimenko, *J. Am. Chem. Soc.* 91 (1969) 3183.
- [15] (a) A. Albinati, R.W. Kunz, C.J. Ammann, P.S. Pregosin, *Organometallics* 10 (1991) 1800. (b) A. Gogoll, J. Örnebro, J.-E. Bäckvall, *J. Am. Chem. Soc.* 116 (1994) 3631.
- [16] (a) B. Crociani, F. Di Bianca, A. Giovenco, T. Bozchi, *Inorg. Chim. Acta* 127 (1987) 169. (b) S. Hansson, P.O. Norrby, M.P.T. Sjögren, B. Åkermark, M.E. Cucciolito, F. Giorjuno, A. Vitagliano, *Organometallics* 12 (1993) 4949.
- [17] Recent examples of restricted rotation about the M-C bond: (a) A.C. Albéniz, A.L. Casado, P. Espinet, *Organometallics* 16 (1997) 5416. (b) J.A. Casares, S. Coco, P. Espinet, Y.S. Lin, *Organometallics* 14 (1995) 3058. (c) G.B. Deacon, E.T. Lawrenz, T.W. Hambley, S. Rainone, L.K. Webster, *J. Organomet. Chem.* 493 (1995) 205. (d) M.J. Sarsfield, S.W. Ewart, T.L. Tremblay, A.W. Roszak, M.C. Baird, *J. Chem. Soc. Dalton Trans.* (1997) 3097. (e) J.A. Casares, P. Espinet, J.M. Martínez de Ilarduya, Y.S. Lin, *Organometallics* 16 (1997) 770. (f) J.A. Casares, P. Espinet, *Inorg. Chem.* 36 (1997) 5428. (g) J.M. Brown, J. Pérez-Torrente, N. Alcock, *Organometallics* 14 (1995) 1195.
- [18] (a) W.T. Dent, R. Long, G. Wilkinson, *J. Chem. Soc.* (1964) 1585. (b) Y. Tatsuno, T. Yoshida, Seiotsuha, *Inorg. Synth.* 19 (1979) 220.
- [19] P. Espinet, J.M. Martínez-de Ilarduya, C. Pérez-Briso, A.L. Casado, M.A. Alonso, *J. Organomet. Chem.* 551 (1998) 9.
- [20] (a) J. Chatt, L.M. Vallarino, L.M. Venanzi, *J. Chem. Soc.* (1957) 3413. (b) D. Drew, J.R. Doyle, *Inorg. Synth.* 13 (1972) 52.
- [21] R.E. Rülke, J.M. Ernsting, A.L. Speck, C.J. Elsevier, P.W.N. van Leewen, R. Vrieze, *Inorg. Chem.* 32 (1993) 5769.
- [22] B.B. Wayland, R.F. Schramm, *Inorg. Chem.* 8 (1969) 971.
- [23] J. Sandström, *Dynamic NMR Spectroscopy*, Academic Press, London, 1982.
- [24] G.M. Sheldrick, *Program for the Refinement of Crystal Structures from Diffraction data*, University of Göttingen, Göttingen, Germany, 1997.
- [25] A. Altomare, G. Cascarano, C. Giacovazzo, A. Guagliardi, M.C. Burla, G. Polidori, M. Camalli, *J. Appl. Cryst.* (1994) 435.